Available online at www.sciencedirect.com
ScienceDirect
Ceramics International 35 (2009) 99–104
CERAMICS INTERNATIONAL
www.elsevier.com/locate/ceramint

# Simultaneous synthesis and consolidation of nanostructured $TaSi_2$–$Si_3N_4$ composite by pulsed current activated combustion

Hyun-Kuk Park [a], Jeong-Hwan Park [a], Jin-Kook Yoon [b], In-Yong Ko [a], Jung-Mann Doh [b], In-Jin Shon [a,*]

[a] *Department of Materials Engineering, Research Center of Advanced Material Development, Chonbuk National University, 664-14 Deokjin-dong 1-ga, Deokjin-gu, Jeonju, Jeonbuk 561-756, South Korea*
[b] *Metal Processing Research Center, Korea Institute of Science and Technology, P.O. Box 131, Cheongryang, Seoul 136-791, South Korea*

Received 9 July 2007; received in revised form 13 August 2007; accepted 28 September 2007
Available online 24 January 2008

**Abstract**

Dense nanostructured $4TaSi_2$–$Si_3N_4$ composite was synthesized by pulsed current activated combustion synthesis (PCACS) method within 3 min in one step from mechanically activated powders of TaN and Si. Simultaneous combustion synthesis and densification were accomplished under the combined effects of a pulsed current and mechanical pressure. Highly dense $4TaSi_2$–$Si_3N_4$ composite with relative density of up to 98% was produced under simultaneous application of a 60 MPa pressure and the pulsed current. The average grain size and mechanical properties (hardness and fracture toughness) of the composite were investigated.


*Keywords:* Pulsed current activated combustion; Intermetallic; Nanophase; $TaSi_2$–$Si_3N_4$

## 1. Introduction

An increase in operating temperature of a gas turbine engine will bring us reductions in both fuel consumption and $CO_2$ emissions. It requires ultra-high temperature structural materials which overwhelm the performance of nickel-based superalloys commercially used as turbine blade and rotors. Among candidate materials based on refractory metal elements, refractory metal silicides seem to have an advantage in oxidation resistance at very high temperatures besides high-elevated temperature strength. Furthermore, the disilicides, in particular $TaSi_2$, $TiSi_2$, $MoSi_2$, $NbSi_2$, and $WSi_2$, have been used as Schottky barriers, ohmic contacts, gate materials, and interconnectors in intergrated circuits, as a result of their low electrical resistivity, high stability, and good compatibility with silicon substrates [1,2]. However, as in the case of many intermetallic compounds, the current concern about these materials focuses on their low fracture toughness below the ductile–brittle transition temperature [3,4]. To improve on their mechanical properties, the approach commonly utilized has been the addition of a second phase to form composites [5–7]. An example is the addition of $Si_3N_4$ to $TaSi_2$ to improve the latter's properties. Silicon nitride has a high thermal shock resistance, due to its low thermal expansion coefficient, and a good resistance to oxidation when compared to other structural materials [8,9]. The isothermal oxidation resistance of $NbSi_2$–40 vol.% $Si_3N_4$ composite prepared by spark plasma sintering (SPS) process in dry air at 1300 °C was superior to that of monolithic $NbSi_2$ compact since the composite contained a larger amount of Si, which made it easier to form dense $SiO_2$ scale [10]. Therefore, $Si_3N_4$ may be the most promising additive as a reinforcing material for $NbSi_2$-based composites.

The method of field-activated and pressure-assisted combustion synthesis has been successfully employed to synthesize and densify materials from the elements in one step in a relatively short period of time. This method has been used to synthesize a variety of ceramics and composites, including $MoSi_2$–$ZrO_2$, $Ti_5Si_3$ and its composites, $WSi_2$ and its composites, and WC–Co hard materials [11–16]. These materials, which are generally characterized by low adiabatic combustion temperature, cannot be synthesized directly by the self-propagating high-temperature synthesis (SHS) method.

* Corresponding author.
*E-mail address:* ijshon@chonbuk.ac.kr (I.-J. Shon).

0272-8842/$34.00 
doi:10.1016/j.ceramint.2007.09.116

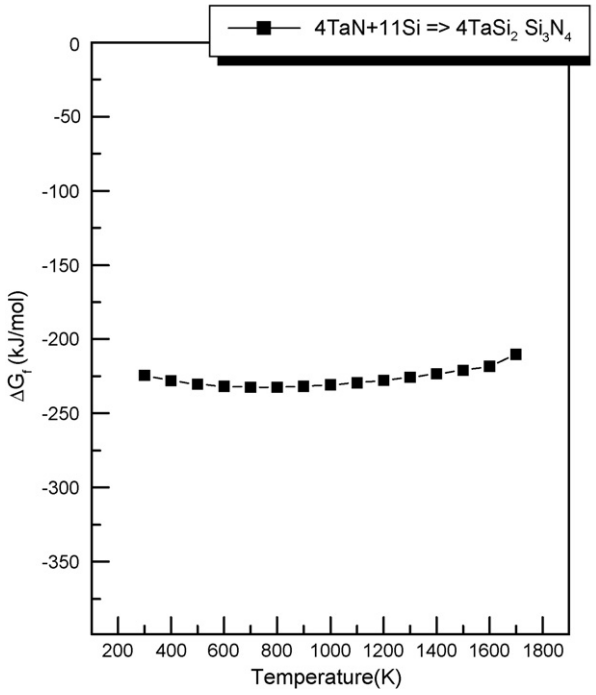


Fig. 1. Temperature dependence of the Gibbs free energy variation by interaction of Ta-nitride (TaN) with silicon.

The objective of this study is to investigate the preparation of dense nanophase $4TaSi_2$–$Si_3N_4$ composite by the pulsed current activated combustion synthesis (PCACS) method starting from a mixture of mechanically activated TaN and Si powders. The interaction between these phases, i.e.,

$$4TaN + 11Si \rightarrow 4TaSi_2 + Si_3N_4 \quad (1)$$

is thermodynamically feasible, as can be seen from Fig. 1.

## 2. Experimental procedure

Powders of 99.97% pure tantalum nitride (−325 mesh, Alfa Products, Ward Hill, MA) and 99% pure silicon (−325 mesh, Aldrich Products, Milwaukee, WI) were used as starting materials. Fig. 2 shows the scanning electron microscopy (SEM) images of the raw materials used. Powder mixtures of TaN and Si in the molar proportion of 4:11 were first milled in a high-energy ball mill (Pulverisette-5, planetary mill) at 250 rpm for 10 h. Tungsten carbide balls (5 mm in diameter) were used in a sealed cylindrical stainless steel vial under argon atmosphere. The weight ratio of ball-to-powder was 30:1. Milling resulted in a significant reduction of grain size. The grain size and the internal strain were calculated by Stokes and Wilson's formula [17]

$$b = b_d + b_e = \frac{k\lambda}{d\cos\theta} + 4\varepsilon\tan\theta \quad (2)$$

where $b$ is the full width at half-maximum (FWHM) of the diffraction peak after instrument correction, $b_d$ and $b_e$ the FWHM caused by small grain size and internal stress, respectively, $k$ the constant (with a value of 0.9), $\lambda$ the wavelength of the X-ray radiation, $d$ and $\varepsilon$ the grain size and internal stress,

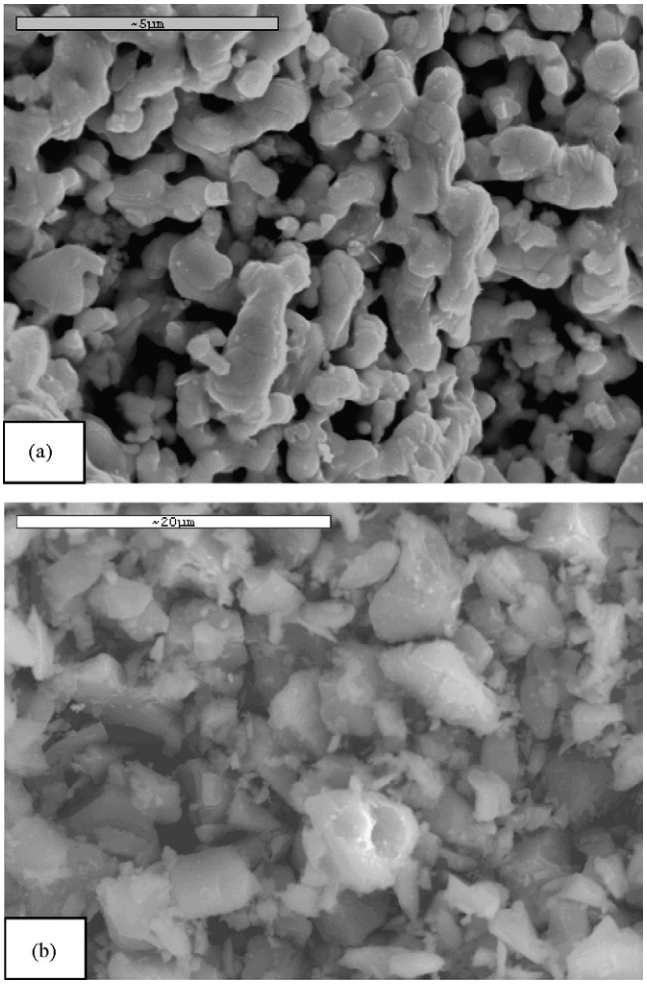


Fig. 2. Scanning electron microscope images of raw materials: (a) tantalum nitride and (b) silicon powder.

respectively and $\theta$ is the Bragg angle. The parameters $b$ and $b_s$ follow Cauchy's form with the relationship: $B_0 = b + b_s$, where $B_0$ and $b_s$ are FWHM of the broadened Bragg peaks and the standard sample's Bragg peaks, respectively. Fig. 3 shows X-ray diffraction (XRD) patterns of the raw powders and the milled 4TaN + 11Si powder mixture. The FWHM of the milled powder is greater than that of the raw powders due to internal strain and grain size reduction. The average grain sizes of the milled TaN and Si powders were determined as 68 and 37 nm, respectively.

After milling, the mixed powders were placed in a graphite die (outside diameter, 45 mm; inside diameter, 20 mm; height, 40 mm) and then introduced into the pulsed current activated combustion sythesis system made by Eltek Co. in Republic of Korea. Schematic diagrams of this method are shown in Fig. 4. The system was first evacuated and a uniaxial pressure of 60 MPa was applied. The PCACS apparatus includes an 18 V, 2800 A dc power supply (which provides a pulsed current with 20 μs on time and 10 μs off time through the sample and die) and a 50 kN uniaxial press. A dc pulsed current was then activated and maintained until the densification rate was negligible, as indicating by the observed shrinkage of the sample. Sample shrinkage is measured in real time by a linear

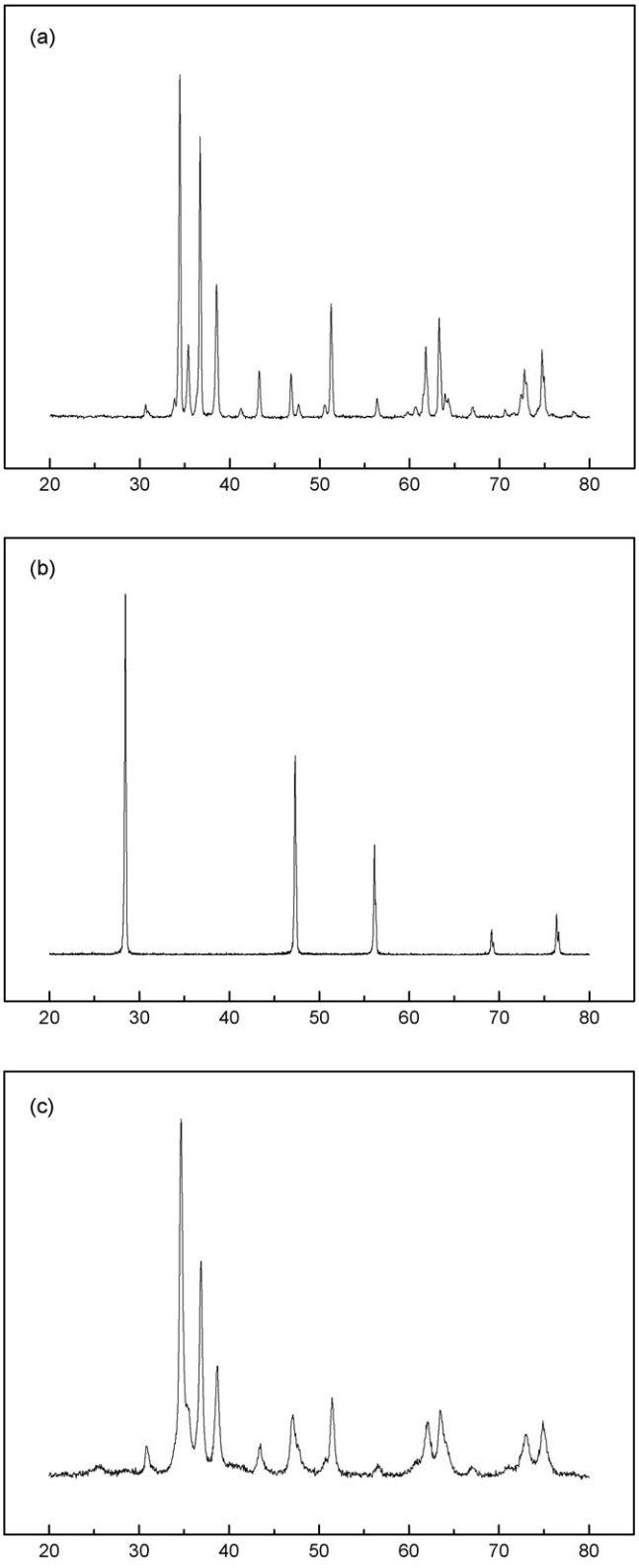


Fig. 3. XRD patterns of raw materials: (a) TaN, (b) Si and (c) milled 4TaN + 11Si.

gauge measuring the vertical displacement. Temperatures were measured by a pyrometer focused on the surface of the graphite die. Depending on heating rate, the electrical and thermal conductivities of the compact, and on its relative density, a

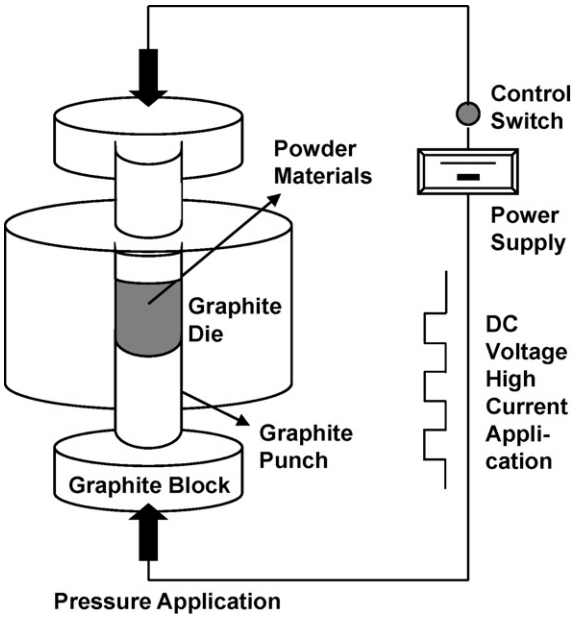


Fig. 4. Schematic diagram of the pulsed current activated combustion apparatus.

difference in temperature between the surface and the center of the sample exists. The heating rates were approximately 600 °C/min in the process. At the end of the process, the pulsed current was turned off and the sample was allowed to cool to room temperature. The entire process of densification using the PCACS technique consists of four major control stages. These are chamber evacuation, pressure application, power application, and cool down. The process was carried out under a vacuum of 40 mTorr.

The relative densities of the synthesized sample were measured by the Archimedes method. Microstructural characterization was made on product samples which had been polished and etched using a solution of HF (30 vol.%), $HNO_3$ (30 vol.%) and $H_2O$ (40 vol.%) for 3 s at room temperature. Compositional and microstructural analyses of the products were made through X-ray diffraction and scanning electron microscopy with energy dispersive X-ray analysis (EDAX). Vickers hardness was measured by performing indentations at a load of 5 kg and a dwell time of 15 s.

## 3. Results and discussion

The variations in shrinkage displacement and temperature with heating time during the processing of 4TaN + 11Si system are shown in Fig. 5. As the pulsed current was applied the specimen showed initially a small (thermal) expansion and then abruptly increased at about 850 °C. When the reactant mixture of 4TaN + 11Si was heated under 60 MPa pressure to 800 °C, no reaction took place and no significant shrinkage displacement as judged by subsequent XRD and SEM analyses. Fig. 6(a)–(c) shows the SEM (secondary electron) images of (a) powder after milling, (b) sample heated to 800 °C and (c) sample heated to 1050 °C, respectively. Fig. 6(a) and (b) shows the presence of the reactants as separate phases. X-ray

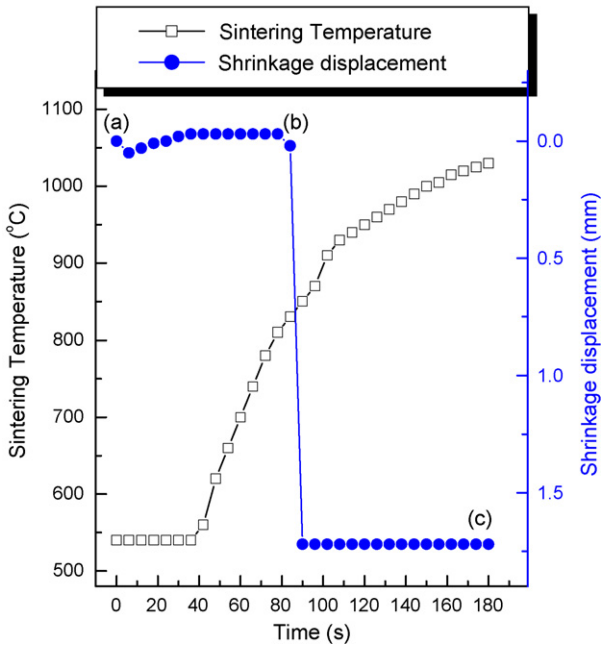


Fig. 5. Variations of temperature and shrinkage displacement with heating time during pulsed current activated combustion synthesis and densification of $TaSi_2$–$Si_3N_4$ composite (under 60 MPa, 2800 A).

diffraction results, shown in Fig. 7(a) and (b) exhibit only peaks pertaining to the reactants TaN and Si. However, when the temperature was raised to 1050 °C, the starting powders reacted producing highly dense products. SEM image of an etched surface of the samples heated to 1050 °C under a pressure of 60 MPa is shown in Fig. 6(c). A complete reaction between TaN and Si took place under these conditions. X-ray diffraction analyses of this sample showed peaks of only $TaSi_2$ and $Si_3N_4$, as indicated in Fig. 7(c). The abrupt increase in the shrinkage displacement at the ignition temperature is due to the increase in density as a result of molar volume change associated with the formation of $4TaSi_2$–$Si_3N_4$ from the reactants (TaN and Si) and the consolidation of the product. It should be recalled that the measured temperatures are those of the surface of the die and are, therefore, likely to be different than the values in the middle of the sample. Thus, the onset of the reaction to form the composite (and the concomitant rapid shrinkage) may be at a higher temperature than the observed value of 850 °C.

The average grain sizes of $TaSi_2$ and $Si_3N_4$ calculated by the Stokes–Wilson formula [17] were about 160 and 70 nm. The $Si_3N_4$ particles were well distributed in matrix, as can be seen from the SEM image, Fig. 6(c).

Vickers hardness measurements were made on polished sections of the $TaSi_2$–$Si_3N_4$ composite using a 5 kg load and 15 s dwell time. The calculated hardness value, based on an average of five measurements, of the $TaSi_2$–$Si_3N_4$ composite is 920 kg/mm$^2$. Indentations with large enough loads produced median cracks around the indent. The length of these cracks permits an estimation of the fracture toughness of the materials by two expressions. The first expression, proposed by Anstis

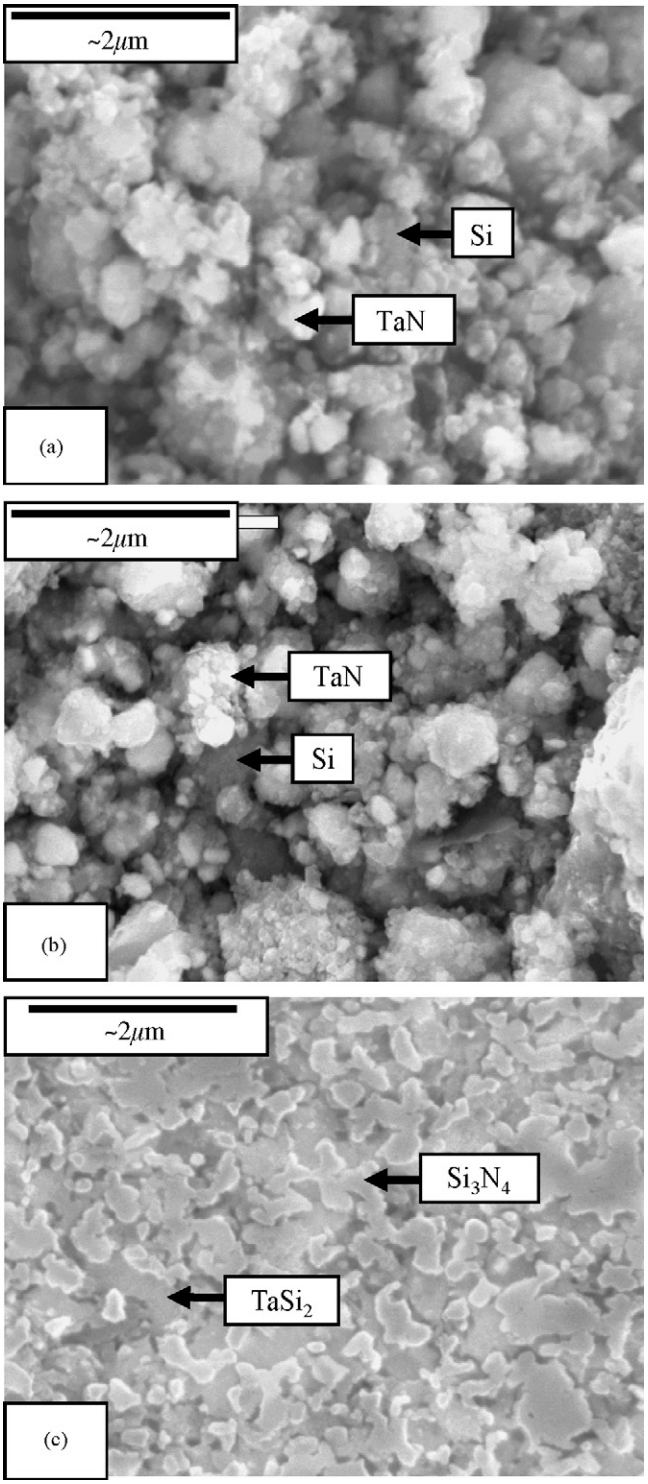


Fig. 6. Scanning electron microscope images of 4TaN + 11Si system: (a) after milling, (b) before combustion synthesis and (c) after combustion synthesis.

et al. [18] is

$$K_{IC} = \frac{0.016(E/H)^{1/2}P}{C^{3/2}} \quad (3)$$

where $E$ is Young's modulus, $H$ the indentation hardness, $P$ the indentation load and $C$ is the trace length of the crack measured

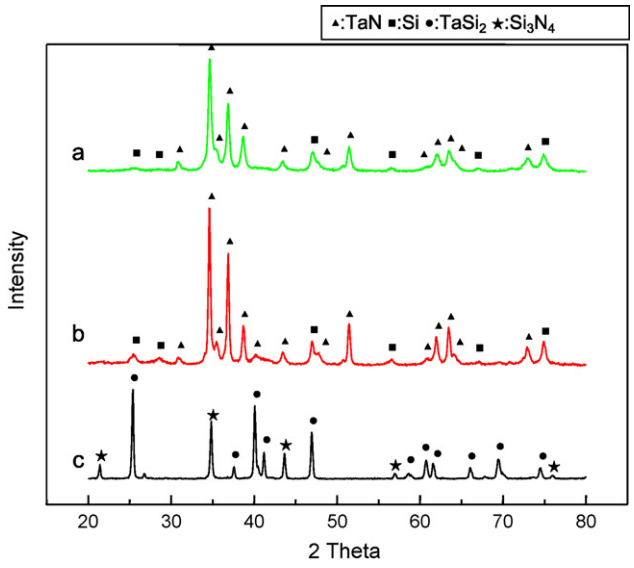


Fig. 7. XRD patterns of the 4TaN + 11Si system: (a) after milling, (b) before combustion synthesis and (c) after combustion synthesis.

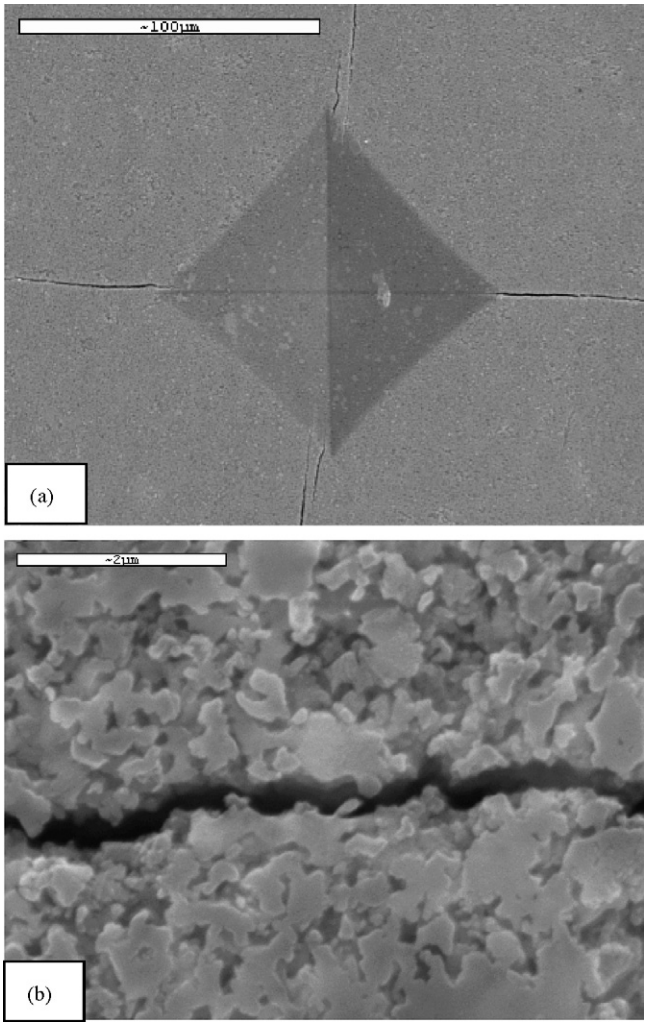


Fig. 8. (a) Vickers hardness indentation and (b) median crack propagating of $TaSi_2$–$Si_3N_4$.

from the center of the indentation. The modulus was estimated by the rule mixtures for the 0.129 volume fraction of $Si_3N_4$ and the 0.871 volume fraction of $TaSi_2$ using $E(Si_3N_4) = 308$ GPa [19] and $E(TaSi_2) = 357$ GPa [20]. The calculated fracture toughness value of $TaSi_2$–$Si_3N_4$ composite is about 4.7 MPa $m^{1/2}$. The second expression, proposed by Niihara et al. [6,21] is

$$K_{IC} = 0.204(c/a)^{-3/2} H_v a^{1/2} \quad (4)$$

where $c$ is the trace length of the crack measured from the center of the indentation, $a$ the half of average length of two indent diagonals and $H_v$ is the hardness. The calculated fracture toughness value of $4TaSi_2$–$Si_3N_4$ composite is about 4.4 MPa $m^{1/2}$. A typical indentation pattern for the $4TaSi_2$–$Si_3N_4$ composite is shown in Fig. 8(a). Typically, one to three additional cracks were observed to propagate from the indentation corner. Higher magnification view of the indentation median crack in the composite is shown in Fig. 8(b). This shows the crack propagates along phase boundary of $TaSi_2$ and $Si_3N_4$.

The absence of reported values for hardness and toughness on $4TaSi_2$–$Si_3N_4$ precludes making direct comparison to the results obtained in this work to show the influence of grain size. Similarly, an absence of corresponding data on $TaSi_2$ makes it difficult to show the effect of the addition of $Si_3N_4$.

## 4. Summary

Using the pulsed current activated combustion method, the simultaneous synthesis and densification of nanostructured $4TaSi_2$–SiC composite was accomplished using powders of TaN and Si. Complete synthesis and densification can be achieved in one step within 3 min. The relative density of the composite was 98% under an applied pressure of 60 MPa and the pulsed current. The average grain sizes of $TaSi_2$ and $Si_3N_4$ phases in the composite were about 160 and 70 nm, respectively. The average hardness and fracture toughness values obtained were 920 kg/$mm^2$ and 4.7 MPa $m^{1/2}$, respectively.

## Acknowledgements

We are grateful for the financial support from the Korea Institute of Science and Technology, which was provided through the program for study on Technologies for Formation and Evaluation of Nano-Structured Composite Coatings.

## References

[1] M.E. Schlesinger, Thermodynamics of solid transition-metal silicides, Chem. Rev. 90 (1990) 607–628.
[2] A.K. Vasudevan, J.J. Petrovic, A comparative overview of molybdenum disilicide composites, Mater. Sci. Eng. A 155 (1992) 1–17.
[3] Y. Ohya, M.J. Hoffmann, G. Petzow, Mechanical properties of hot-pressed SiC-$TiB_2$/TiC composites synthesized in situ, J. Mater. Sci. Lett. 12 (1993) 149–152.
[4] J. Qian, L.L. Daemen, Y. Zhao, Hardness and fracture toughness of moissanite, Diamond Related Mater. 14 (2005) 1669–1672.

[5] Y. Ohya, M.J. Hoffmann, G. Petzow, Sintering of in-situ synthesized Sic–$TiB_2$ composites with improved fracture toughness, J. Am. Ceram. Soc. 75 (1992) 2479–2483.
[6] D.Y. Oh, H.C. Kim, J.K. Yoon, I.J. Shon, One step synthesis of dense $MoSi_2$–SiC composite by high-frequency induction heated combustion and its mechanical properties, J. Alloys Compd. 395 (2005) 174–180.
[7] S.K. Bhaumik, C. Divakar, A.K. Singh, G.S. Upadhyaya, Synthesis and sintering of $TiB_2$ and $TiB_2$–TiC composite under high pressure, Mater. Sci. Eng. A 279 (2000) 275–281.
[8] W. Dressler, R. Riedel, Progress in silicon-based non-oxide structural ceramics, Int. J. Refract. Met. Hard Mater. 15 (1997) 13–47.
[9] S.P. Taguchi, S. Ribeiro, Silicon nitride oxidation behaviour at 1000 and 1200 °C, J. Mater. Process. Technol. 147 (2004) 336–342.
[10] T. Murakami, S. Sasaki, K. Ichikawa, A. Kitahara, Microstructure, mechanical properties and oxidation behavior of Nb–Si–Al and Nb–Si–N powder compacts prepared by spark plasma sintering, Intermetallics 9 (2001) 621–628.
[11] Z.A. Munir, I.J. Shon, K.Yamazaki, U.S. Patent No. 5,794,113 (1998).
[12] I.J. Shon, Z.A. Munir, K. Yamazaki, K. Shoda, Simultaneous synthesis and densification of $MoSi_2$ by field-activated combustion, J. Am. Ceram. Soc. 79 (1996) 1875–1880.
[13] I.J. Shon, H.C. Kim, D.H. Rho, Z.A. Munir, Simultaneous synthesis and densification of $Ti_5Si_3$ and $Ti_5Si_3$–20 vol% $ZrO_2$ composites by field-activated and pressure-assisted combustion, Mater. Sci. Eng. A 269 (1999) 129–135.
[14] I.J. Shon, D.H. Rho, H.C. Kim, Z.A. Munir, Dense $WSi_2$ and $WSi_2$–20 vol.% $ZrO_2$ composite synthesized by pressure-assisted field-activated combustion, J. Alloys Compd. 322 (2001) 120–126.
[15] I.J. Shon, D.H. Rho, H.C. Kim, Simultaneous synthesis and densification of $WSi_2$ and $WSi_2$–20 vol%Nb composite by field-activated and pressure-assisted combustion, Met. Mater. 6 (2000) 533–541.
[16] C.D. Park, H.C. Kim, I.J. Shon, Z.A. Munir, One-step synthesis of dense tungsten carbide-cobalt hard materials, J. Am. Ceram. Soc. 85 (2002) 2670–2677.
[17] F.L. Zhang, C.Y. Wang, M. Zhu, Nanostructures WC/Co composite powder prepared by high energy ball milling, Scripta Mater. 49 (2003) 1123–1128.
[18] G.R. Anstis, P. Chantikul, B.R. Lawn, D.B. Marshall, A critical evaluation of indentation techniques for measuring fracture toughness. I. Direct crack measurements, J. Am. Ceram. Soc. 64 (1981) 533–538.
[19] M. Lugovy, V. Slyunyayev, V. Subbotin, N. Orlovskaya, G. Gogotsi, Crack arrest in $Si_3N_4$-based layered composites with residual stress, Compos. Sci. Technol. 64 (2004) 1947.
[20] F. Chu, M. Lei, S.A. Maloy, J.J. Petrovic, T.E. Mitchell, Elastic properties of C40 transition metal disilicides, Acta Mater. 44 (1996) 3035.
[21] K. Niihara, R. Morena, D.P.H. Hasselman, Evaluation of KIC of brittle solids by the indentation method with low crack-to-indent ratios, J. Mater. Sci. Lett. 1 (1982) 12–16.